PAPER

Check for updates

A selective and sensitive nanosensor for fluorescent detection of specific IgEs to purified allergens in human serum

Jianrong Yun, [a] Fang Duan, [c] Liming Liu, [b] Xiulai Chen, [b] Jia Liu, [b] Qiuling Luo [b] and Jing Wu *[ab]

Food allergies are increasingly recognized as a major healthcare concern. In order to sensitively and specifically detect allergies from blood samples of at-risk allergic patients, an effective magnetic fluorescence sensing platform (EMFP) was constructed. The EMFP incorporated hollow mesoporous silica nanospheres (HMNs) to amplify signal from the target IgE in addition to magnetic nanoparticles (MNPs) to capture and separate the target IgE. The application of EMFP to immunoassays indicated a detection limit of 0.0159 ng mL^{-1} for low concentration specific immunoglobulin E (sIgE) against purified shellfish *Metapenaeus ensis* (Meta. E.) allergens, which is 15 fold more sensitive than the commercially available Food and Drug Administration-approved analyzers. Notably, EMFP was specific for the targeted sIgE even with interference by other sIgEs. In addition, the detection time is only 75 min, considerably faster than current commercial ELISA kits for IgE assays. Together, these results demonstrated that EMFP has excellent sensitivity and selectivity for the rapid detection of sIgE. The method thus exhibits potential toward the rapid monitoring of sIgE against Meta. E. allergens in clinical application.

Introduction

The prevalence of food allergy reactions, which range in severity from relatively mild features to life-threatening anaphylaxis, has been estimated as affecting up to 7% of children and 6% of adults[1–6] and is currently considered as a global public health problem.[7,8] The clinical diagnosis of food allergy primarily involves skin testing[9,10] and blood (serum) analysis.[11,12] The skin test is performed by carefully observing patient symptom after a handful of possible allergens are laid on or below the skin, whereas the blood test involves detecting the concentration of immunoglobulin E (IgE) against specific allergens in the patient serum.[13] IgE is a glycoprotein that is at almost undetectable levels in normal human serum, whereas its concentration increases notably when the organism is exposed to allergens.[14] In comparison with skin tests, the specific IgE (sIgE) test possesses the following advantages. First, it offers convenience as the preparation of blood tests only involves a standard blood draw.[15,16] Second, the blood test is regarded as safer because the

process is conducted *in vitro*, and thus does not expose patients to allergens.[17,18] Third, the blood tests can serve as an alternative to skin tests for patients who suffer from severe symptoms and cannot interrupt medication.[19] Furthermore, studies have revealed that the number of sIgE detected against allergens is able to predict the extent of allergy symptoms.[20–22]

Several current methods are available to determine sIgEs in serum including radioimmunometric assays, commercial analyzer systems, or enzyme-linked immunosorbent assays (ELISA).[23–26] Although the detection limit of the radio-immunometric assay is very low (0.05 ng mL^{-1}),[26] using radio-active reagents constitutes a serious drawback. The commercial autoanalyzer system (the ImmunoCAP ISAC assay, Phadia) employed to determine sIgE possesses a published lowest detection limit of only 0.24 ng mL,[23] and the detection cost is usually fairly expensive for most patients. The ELISA tends to be laborious and requires highly trained personnel and numerous operation steps, thereby failing to allow the timely design of treatments to prevent allergic patients from life-threatening events.[24,25] Recently, nanomaterials have increasingly been used for food allergy detection.[27–30] Although the detection limit for the application of photonic crystal enhanced fluorescence toward detection of sIgE is very low (0.048 ng mL^{-1}),[30] the detection procedures are cumbersome, and substantial, expensive equipment is required, which limit its clinical application. Gold nanoclusters as fluorescent labels for the determination of total IgE is more convenient and simple,

[a]School of Pharmaceutical Sciences, Jiangnan University, 1800 Lihu Road, Wuxi 214122, Jiangsu Province, P. R. China. E-mail: wujing@jiangnan.edu.cn; Fax: +86-510-85197873; Tel: +86-510-85197873

[b]The Key Laboratory of Industrial Biotechnology, Ministry of Education, Jiangnan University, Wuxi 214122, Jiangsu Province, P. R. China

[c]School of Chemical and Material Engineering, Jiangnan University, Wuxi 214122, Jiangsu Province, P. R. China

however, the detection limit is 0.2 ng mL^{-1} which does not provide adequate levels of sensitivity, and the test results do not suggest which allergen may be mediating the allergic reaction.[28] Therefore, there is a pressing need to develop new techniques for the rapid, low-cost, and sensitive detection of sIgEs.

Notably, the development of previous systems of sIgE detection depended on the use of crude allergen extracts from biological materials. However, it is often difficult to normalize for allergen content and isolation efficiency.[31] Thus, an optimal detection method should be calibrated against purified allergens prior to testing using actual biological samples. One likely option would be shellfish, as one of the eight major food allergens responsible for most anaphylactic reactions owing to its economic and nutritional value.[32,33]

In order to solve the problems of low sensitivity, time-requirements, and interminable operation steps in the process of testing sIgE, the strategies of signal amplification and rapid target enrichment were adopted in this study. We synthesized hollow mesoporous materials as an efficient strategy in signal amplification to improve sensitivity. Magnetic nanoparticles (MNPs) were synthesized to separate and enrich the target sIgE to simplify operations and allow rapid detection. Proper carbodiimide conjugation was utilized to generate fluorescent immune particles (HMNs@PDDA@PAA-anti-IgE) and magnetic immune particles (Fe$_3$O$_4$@SiO$_2$@PAA-allergens). Integrating the two materials permitted the development of an efficient magnetic fluorescence platform (EMFP). Taking sIgE against the shellfish *Metapenaeus ensis* (Meta. E.) as a study model, a new and simple fluorescence sensor was developed with the characteristics of easy operation along with rapid and sensitive detection.

Experimental

Chemicals and instruments

All chemicals were purchased from Aldrich (St. Louis, MO, USA) unless otherwise stated. Tetraethoxysilane (TEOS, >99.9%), cetyl trimethyl ammonium bromide (CTAB, >99.0%), polystyrene (PS, 5 wt% in water), iron oxide (Fe$_3$O$_4$, 99.5% metals basis), ammonium hydroxide solution (28 wt%), and hydrochloric acid (36 wt%), (N-(3-dimethylaminopropyl)-N'-ethyl-carbodiimide) (EDC, >99.0%), 1-hydroxy-5-pyrrolidinedione (NHS, 98.0%), fluorescein 5(6)-isothiocyanate (FITC, 95%), poly dimethyl diallyl ammonium chloride (PDDA, 60 wt%), polyacrylic acid (PAA, MW-2000), 4-dimethylaminopyridine (DMAP, 99.0%), dicyclohexylcarbodiimide (DCC, 99.0%), N,N-dimethylformamide (DMF, 98.0%), blocking buffer (Beyotime, Shanghai, China), and Tween-20. Deionized water was generated using a Milli-Q integral pure and ultrapure water purification system (Millipore, Billerica, MA, USA). The human IgE ELISA Kit was purchased from Multi Sciences (Lian Ke) Biotech, Co., Ltd. (Hang Zhou, China).

The following equipment was used for sample characterization. Fourier transform infrared (FTIR) instrument (Bruker Vertex 70 FTIR, Karlsruhe, Germany) (400–4000 cm^{-1}, KBr pellet technique), an X-ray diffractometer (Rigaku D/Max-Ra, Tokyo, Japan) ($\lambda = 1.5418$ Å) to record X-ray diffraction (XRD) curves,

and sample morphology was analyzed with a transmission electron microscope (TEM) (JEOL JEM-2100, Tokyo, Japan). Vibrating sample magnetometry (VSM) (Lake Shore 7410, Houston, USA) was applied to record sample magnetic features. Emission spectra were recorded using a fluorescence spectrophotometer (Hitachi F-4500, Tokyo, Japan).

Source of materials

We evaluated the feasibility of EMFP for the sensitive and selective determination of allergen-specific IgE; the two recombinant purified major allergens tropomyosin and arginine kinase produced by *Escherichia coli*, and Meta. E. extract were employed. The human sera used in these studies were provided by Wuxi the Fourth People's Hospital, which were clinically tested as representing true negative and positive samples with a standard clinical analyzer used for allergy testing (ELISA).

Preparation of hollow mesoporous silica nanospheres (HMNs)

HMNs were prepared following previously established methodology with some modifications.[34] Briefly, 0.30 g CTAB was dissolved in a mixture of 1.0 mL ammonium hydroxide solution, 12 g ethanol, and 29 g water. Then, 500 μL of 5% PS was added dropwise to the above CTAB solution at room temperature with vigorous stirring and subsequently sonicated for 20 min. The milky mixture was then magnetically agitated for 30 min before injecting 120 μL of TEOS inchwise. The mixture was kept at room temperature for 24 h before the mesoporous silica-coated latex was harvested by centrifugation at 6000g for 5 min. The precipitate was washed with numerous copious amounts of ethanol and then dried at 45 °C. Finally the material was calcined in air at 600 °C for 5 h using a heating rate at 3 °C min^{-1} to form HMNs.

Preparation of immunolabels of FHMNs@polymers-anti-IgE

In order to obtain the immuno labels, 0.04 g of HMNs and 0.012 g of FITC were added to 5 mL deionized water. The mixture was stirred at room temperature for 48 h before centrifuging and drying the compounds at 45 °C. Then, 10 mg of FHMNs were immersed in 0.20% PDDA aqueous solution with stirring for 30 min to produce a homogeneous suspension. The remaining PDDA was then removed by washing with deionized water *via* centrifugation, and subsequently the compound was immersed in a 0.50% PAA solution with stirring for approximately 30 min.[35] The remaining PAA polymer was removed by centrifuging at high speed. The obtained nanospheres were further self-assembled with PDDA and PAA by repeating the steps above. The eventual nanocomposites (FHMNs@polymers) fulfilled the necessary requirement of preserving the internal fluorescein dye molecule from leakage; this property was confirmed using ultraviolet and fluorescence spectrum analysis of the supernatant after centrifugation. The number of fluorescein molecules stored in the FHMNs@polymers was judged by testing the fluorescence intensity of the released dye molecules from 10 mg of FHMNs. We obtained the

same content of 37.56% from multiple acquired detections, confirming consistency.

The prepared nanospheres *via* layer-by-layer self-assembly were dispersed into a mixture that contained 0.5 mg mL^{-1} NHS and 1 mg mL^{-1} EDC for 30 min to motivate the carboxyl group of the PAA layer.[36] Subsequently, the nanospheres were rapidly dispersed into anti-IgE antibody (Ab$_2$) solution at 37 °C for 2 h to generate immunolabels of FHMNs@polymers. After collection by centrifugation, the precipitate was washed three times with a washing buffer (PBST) containing 10 mM sodium phosphate, 0.15 M NaCl, and 0.05% (v/v) Tween-20 to remove the remaining antibodies. The remnant immunocompetent domains of the FHMNs@polymers-anti-IgE were blocked with blocking reagent at 37 °C for 1 h. Eventually, after centrifuging the nanocomposites were washed three times with washing buffer (pH 7.4) and stored in PBS (pH 7.4) at 4 °C.

Preparation of magnetic nanoparticles

Fe$_3$O$_4$@SiO$_2$ nanoparticles were prepared according to a previously established method with several modifications.[37] Briefly, 300 mg of Fe$_3$O$_4$ was dispersed into a mixture of 40 mL ethanol and 4 mL H$_2$O. After sonicating the mixture for 15 min, 5 mL ammonia and 2 mL TEOS were added while stirring. The reaction was carried out for 12 h, after which the product was magnetically separated, washed with hydrochloric acid (0.1 mol L^{-1}) and water three times, and then vacuum dried at 60 °C for 10 h. Fe$_3$O$_4$@SiO$_2$@PAA nanospheres were prepared following a previously established procedure. Briefly, 1 g of Fe$_3$O$_4$@SiO$_2$ was dispersed in 33 mL DMF, and this was then mixed with a solution of 2 g PAA dissolved in 33 mL DMF. After sonication for 30 min, the mixture was heated to 110 °C while stirring vigorously. Next, 0.033 g of DMAP (dissolved in 3.3 mL of DMF) and 0.33 g of DCC (dissolved in 6.6 mL of DMF) were added dropwise. The mixture was kept at 110 °C for 12 h while stirring. The products were magnetically separated, washed with ethanol three times, and vacuum dried at 60 °C.

Preparation of magnetic immune probes of Fe$_3$O$_4$@SiO$_2$@PAA-allergens

Fe$_3$O$_4$@SiO$_2$@PAA-allergens immune probes were prepared following established methodology. Briefly, Fe$_3$O$_4$@SiO$_2$@PAA were dispersed in a solution that contained 1 mg mL^{-1} EDC and 0.5 mg mL^{-1} NHS for 30 min. After activation, the Fe$_3$O$_4$@SiO$_2$@PAA was rinsed with PBS (pH 7.4), then immediately dispersed into allergens (Ag) solution for 2 h to yield Fe$_3$O$_4$@SiO$_2$@PAA-allergens. Next, the composite was magnetically washed with PBS three times to remove the residual antibodies. The remaining active sites of Fe$_3$O$_4$@SiO$_2$@PAA-allergens were blocked with blocking buffer at 37 °C for 1 h. The resulting composites were separated and washed with PBS (pH 7.4) three times and stored in 10 mL PBS (pH 7.4) at 4 °C before use.

Bioassay procedure for IgE

The assay procedure was as follows: 0.1 mL of human serum or serum dilution in blocking reagent was incubated with the mixture of 0.1 mL of Fe$_3$O$_4$@SiO$_2$@PAA-antigens and 0.15 mL of

FHMNs@polymers-anti-IgE, next, the mixture was magnetically attracted after being vigorously shaken at 37 °C for some time and the non-magnetic portions were discarded. The magnetic precipitates were carefully washed with wash buffer three times. Lastly, 3 mL of 0.1 mol mL^{-1} sodium hydroxide solution (pH 11) was used to dissolve the HMNs and release the internal fluorescent dye with ultrasonic processing for 10 min. The fluorescence intensity was determined to show the sIgE content.

Results and discussion

Synthesis and characterization of materials

The magnetic beads were utilized as allergen carriers to capture and enrich samples for testing in a one-step process. The Stöber method was used to produce Fe$_3$O$_4$@SiO$_2$,[37] with the silicon source coated on the surface of Fe$_3$O$_4$, followed by covalent binding with PAA to eventually form Fe$_3$O$_4$@SiO$_2$@PAA. The synthesized material was characterized using TEM, FTIR, XRD, and VSM. Fig. 1A shows TEM images of Fe$_3$O$_4$ and Fe$_3$O$_4$@SiO$_2$. Fe$_3$O$_4$ exhibited angular and amorphous particles with different sizes ranging from 7 to 25 nm. Visible aggregation of Fe$_3$O$_4$ was displayed in the TEM image that could be attributed to the strong magneticity. In comparison, Fe$_3$O$_4$@SiO$_2$ particles displayed spherical morphology with a larger average diameter of 110 nm. The FTIR spectra of Fe$_3$O$_4$, Fe$_3$O$_4$@SiO$_2$, and Fe$_3$O$_4$@SiO$_2$@PAA are shown in Fig. 1B. The bands at 1082 cm^{-1} and 957 cm^{-1} could be assigned to Si–O–Si and Si–OH groups,[38] respectively, and the peak intensity at 653 cm^{-1} for Fe–O group decreased significantly (curve b).[39] After adding PAA based on Fe$_3$O$_4$@SiO$_2$, primary absorptions appeared at 1379 cm^{-1} for –OH of the C–OH group, and the peak at 1663 cm^{-1} of the C=C group increased.[40] Given these results, we could confirm that the silica and PAA had well-coated the outer surface of Fe$_3$O$_4$ particles.[40,41]

To examine the magnetic beads structure, the X-ray diffraction patterns for Fe$_3$O$_4$, Fe$_3$O$_4$@SiO$_2$, and Fe$_3$O$_4$@SiO$_2$@PAA were used as shown in Fig. 1C. Compared with Fe$_3$O$_4$, a single characteristic peak at $2\theta \approx 22°$ was displayed in the diffraction peaks of Fe$_3$O$_4$@SiO$_2$ and Fe$_3$O$_4$@SiO$_2$@PAA. The results revealed that SiO$_2$ was successfully grafted onto the Fe$_3$O$_4$ surface and that the amorphous layer did not impact the structure of Fe$_3$O$_4$.[42] The magnetism was analyzed using a magnetometer at room temperature; the results are displayed in Fig. 1D. The saturation intensities for Fe$_3$O$_4$, Fe$_3$O$_4$@SiO$_2$, and Fe$_3$O$_4$@SiO$_2$@PAA were 57.168, 18.234, and 18.164 emu g^{-1}, respectively. This difference was possibly due to the introduction of silica shells to the surface of Fe$_3$O$_4$ nanoparticles, which decreased magneticity. Thus, these observations confirm that we were able to obtain Fe$_3$O$_4$@SiO$_2$@PAA possessing the desired properties.

To amplify signal for low concentration target sIgE, HMNs were prepared using the soft template method.[43] Briefly, silicon source was coated on the surface of template PS during a condensation polymerization, after which calcination decomposition of the PS was performed to form HMNs. The synthesized materials were characterized with TEM and FTIR. TEM images showed that the PS nanospheres had round,
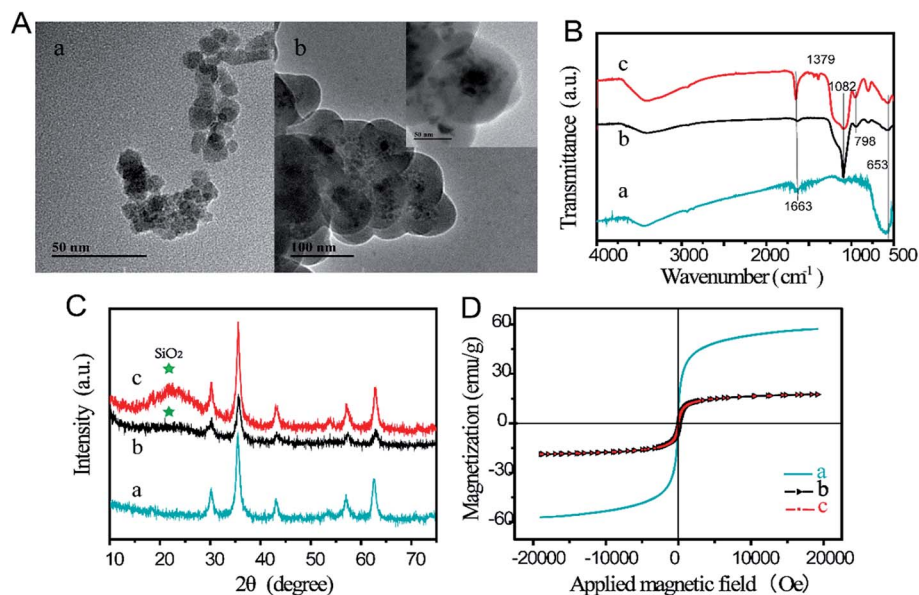
Fig. 1 (A) TEM images of Fe$_3$O$_4$ (a) and Fe$_3$O$_4$@SiO$_2$ (b); (B) FTIR images; (C) XRD images; and (D) magnetic intensity images of Fe$_3$O$_4$, (b) Fe$_3$O$_4$@SiO$_2$, and (c) Fe$_3$O$_4$@SiO$_2$@PAA.

uniform structures with an average diameter of 130 nm as shown in Fig. 2A. Fig. 2B indicates that the hollow structures possessed a mesoporous SiO$_2$ spherical shell with 35 nm thickness. The unique hollow structure and grouping of the HMNs suggest them as attractive candidates for dye molecules. The FTIR of HMNs, FITC, and FHMNs@polymers are shown in Fig. 2C. With the accumulation of FITC molecules and self-assembly of PDDA and PAA, the peaks at 1732 and 1390 cm^{-1} could be ascribed to the C=O stretch vibration and O–H of the C–O–H group,[40,44] respectively; additionally, the band of the C=C group at 1605 cm^{-1} increased whereas the band of Si–O–Si at 1082 cm^{-1} weakened (curve c).[38] These data further demonstrate that FHMNs@polymers were successfully achieved.

Optimization of the detection conditions

The pH of the fluorescein-release solution, incubation temperature, and incubation time plays important roles in the performance of the sensor. First, the effect of pH was investigated, which indicated that the fluorescence intensity reached a maximum value just at pH 11.0, as shown in Fig. 3A. In acidic and neutral environments, the dye molecules were protected by an undissolved SiO$_2$ shell and shrunken polymer layers, allowing no fluorescein leakage. In an alkaline solution of sodium hydroxide, the weaker the alkalinity, the longer the time that was needed to release all of the dye molecules. The fluorescence intensity of the released fluorescein was affected by the acidity, this property may occur because of the structure of FITC. Taking both of these factors into account, a sodium hydroxide solution of pH 11.0 was used to release the fluorescein and as the detection medium. In addition, investigation of the effect of incubation temperature determined that the maximal fluorescence intensity was obtained at 37 °C as shown in Fig. 3B. When the incubation temperature was higher than 37 °C, the intensity of the fluorescence decreased, which may have occurred because of a reduction in biomolecule activity at high temperatures. Investigating the effect of incubation time showed that approximately 85% of fluorescence intensity was obtained at 60 min, when most of the silica was dissolved and a large number of fluorescent molecules were released. Thus, in order
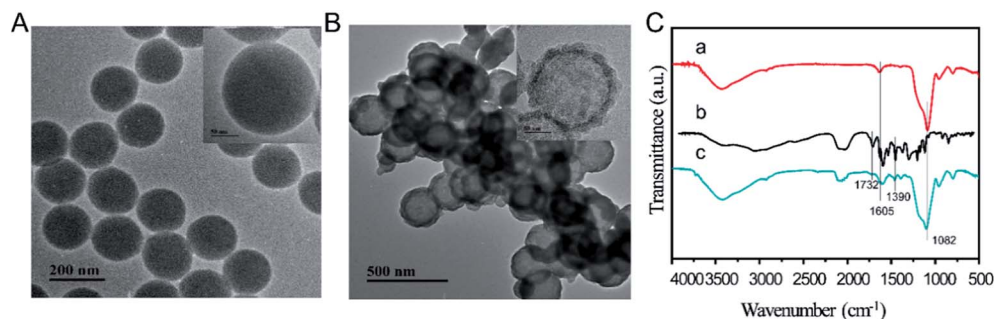

Fig. 2 TEM images of (A) polystyrene nanospheres and (B) HMNs. (C) FTIR of (a) HMNs, (b) FITC, and (c) FHMNs@polymers.
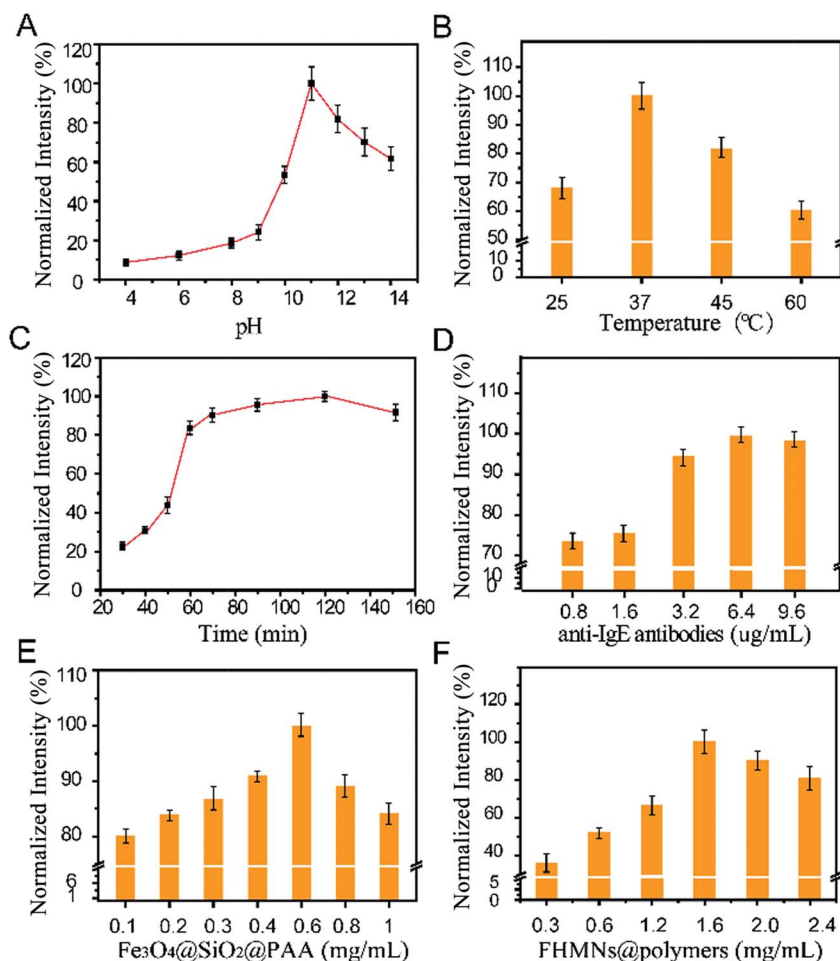
Fig. 3 Effect of pH (A), incubation time (B), incubation temperature (C), concentration of anti-IgE antibodies (D), concentration of $Fe_3O_4@$-$SiO_2@PAA$ (E), and concentration of FHMNs@polymers (F) on fluorescence intensity.

to achieve rapid detection, we adopted 60 min incubation time although subsequently increasing for fluorescence intensity (Fig. 3C). Based the above results, the conditions of pH 11.0, incubation temperature of 37 °C and incubation time of 60 min were employed in the subsequent experiments.

The concentrations of anti-IgE antibodies, $Fe_3O_4@SiO_2@$-PAA, and FHMNs@polymers were optimized as follows. Investigation of the effect of anti-IgE antibody concentration determined that the maximal fluorescence intensity was obtained at 6.4 μg mL^{-1} (Fig. 3D). A low concentration of anti-IgE antibody resulted in lower fluorescence intensity owing to inadequate binding of antibodies, whereas antibody concentration above 6.4 μg mL^{-1} could lead to non-specific binding, which may reduce the sensitivity and specificity of the sensor. In addition, investigation of the effect of $Fe_3O_4@SiO_2@PAA$ concentration determined that the maximal fluorescence intensity was obtained at 0.6 mg mL^{-1} (Fig. 3E). The fluorescence intensity decreased when the concentration of $Fe_3O_4@$-$SiO_2@PAA$ was higher than 0.6 mg mL^{-1} because the excess Fe_3O_4 obtained after dissolution of the silica shell produced a quenching effect.[45] Investigating the effect of FHMNs@polymers concentrations showed that the maximum fluorescence

was exhibited at 1.6 mg mL^{-1} (Fig. 3F). The fluorescence intensity was decreased when the amount of FHMNs@polymers was more than 1.6 mg mL^{-1}, which may have been due to the aggregation-induced quenching effect of fluorescence molecules.[46] In conclusion, the conditions of 6.4 μg mL^{-1} anti-IgE, 0.6 mg mL^{-1} $Fe_3O_4@SiO_2@PAA$, and 1.6 mg mL^{-1} FHMNs@polymers were employed in the subsequent experiments.

Working principles of the sensor

Scheme 1 illustrates the preparation of the EMFP sensor and the working principle of the sensor for detecting and quantifying the target sIgE. The synthesized $Fe_3O_4@SiO_2@PAA$ carried purified allergens (Ag), which captured and separated target sIgEs in a one-step process. In addition, thousands of fluorescein molecules encapsulated in individual protective HMNs along with anti-IgE antibody linked to FHMNs@polymers, together provided a highly amplified signal for fluorescence-based bio-analysis, as the two immune nanocomposites were linked with target sIgEs and functioned simultaneously. These constitute an ideal candidate platform to amplify the signal of low level sIgE and provide rapid enrichment and separation of
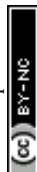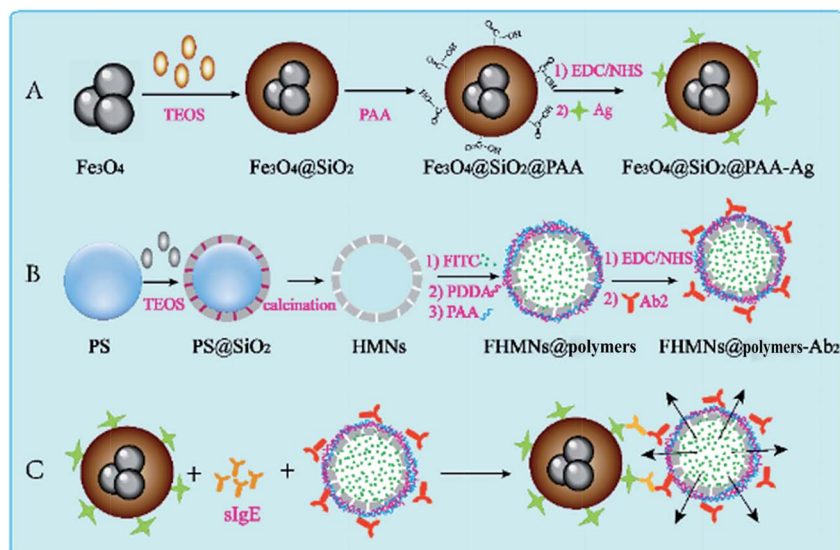
Scheme 1 Schematic of (A) the preparation of magnetic immune probes, (B) the preparation of FHMNs@polymer-Ab$_2$, and (C) the bioassay procedure for target sIgE detection.

target sIgE. Moreover, it is a simple procedure because the conjugation between allergen and antibody requires only one step, and non-specific antibody is separated and removed by only one wash procedure repeated five times. This straightforward assay results in rapid detection and high sensitivity for the target sIgE.
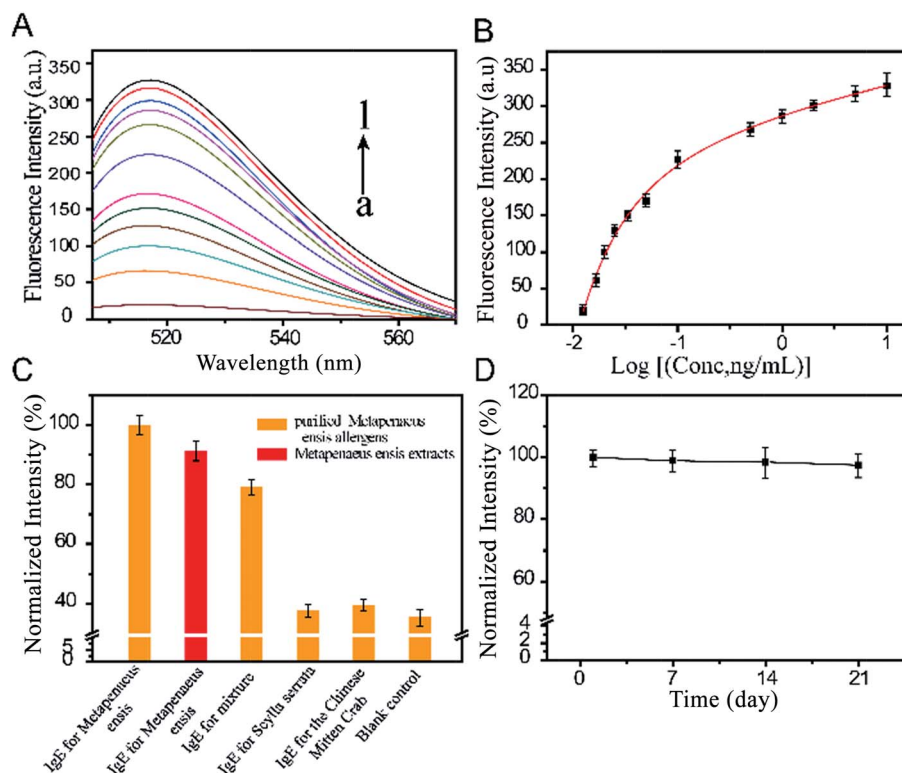

Fig. 4 Characterization of the fluorescent responses of the sensor using sIgE. (A) Fluorescent responses of the sensor using different concentrations of sIgE of Meta. E. (a) 0.0125 ng mL^{-1}, (b) 0.0159 ng mL^{-1}, (c) 0.02 ng mL^{-1}, (d) 0.025 ng mL^{-1}, (e) 0.03333 ng mL^{-1}, (f) 0.05 ng mL^{-1}, (g) 0.10 ng mL^{-1}, (h) 0.50 ng mL^{-1}, (i) 1 ng mL^{-1}, (j) 2 ng mL^{-1}, (k) 5 ng mL^{-1}, (l) 9.895 ng mL^{-1}. (B) The corresponding calibration curve between fluorescent values of released FHMNs and the concentration of sIgE of Meta. E. (other assay conditions were optimized). (C) Fluorescent responses of the sensor in a variety of different sera with purified and crude allergens: sIgE antibodies for Meta. E., *Scylla serrata*, the Chinese mitten crab, and a mixture of sIgEs for these. (D) Fluorescent responses of the sensor by storage time at 4 °C.

Paper RSC Advances

Sensitivity, selectivity, and stability of the sensor

In order to estimate the sensitivity of the sensor, a dose response study was performed with different concentrations of human sera. It can be seen in Fig. 4A that fluorescence intensity (excitation at 517 nm) gradually increased with growing concentration of target sIgE. As shown in Fig. 4B, the fluorescence intensity and concentrations of target sIgE had a correlation coefficient of 0.9959. The good linear relationship ranging from 0.0125 to 9.895 ng mL^{-1}, could be expressed by the regression equation $y = 452 - 164.2 \times 0.7562^x - 1.387 \times 0.0842^x$. This indicated that the fluorescent sensor could be employed to quantize the concentration of the target sIgE. The limit of detection (LOD) (three times the standard deviation above the blank, $n = 6$) of the sensor was as low as 0.0159 ng mL^{-1}, this is lower than the lowest detectable concentration of 0.24 ng mL^{-1} measured by the ImmunoCAP system. The results thus indicate that the sensor is highly sensitive for target sIgEs.

To verify the selectivity of the method, sIgEs was employed including sIgE of Meta. E., the Chinese mitten crab, *Scylla serrata*, and a mixture of sIgE of those with the same concentrations. As shown in Fig. 4C, compared to the blank test, the fluorescence intensity for the presence of the control sIgE (for the Chinese mitten crab and *Scylla serrata*) showed negligible changes, whereas that of the mixture containing target sIgE showed a slight influence compared to the target sIgE. In comparison, purified antigens had higher fluorescence intensities than Meta. E. extract, which demonstrates that purified allergens exhibit stronger binding capacity. These results demonstrated that the proposed sensor showed high selectivity toward sIgE against purified Meta. E. antigens.

Stability was tested by examining the fluorescent signal of the sensor against storage time (Fig. 4D). The fluorescent signal changed only slightly when the bio-conjugated FHMNs and magnetic probes were used after storage at 4 °C for 3 weeks, suggesting the good stability of the sensor, which could be attributed to the well-known biocompatibility of the surface microenvironment for antibody conjugation.

Application of the sensor

To assess the applicability of the sensor, we tested 9 human sera using both ELISA kits and the developed EMFP system. The results are recorded in Table 1. All samples demonstrated higher level by the EMFP system. Notably, the sIgE in serum #6 was only detectable by the EMFP system. These results confirm that the sensor possessed high sensitivity. It also showed good repeatability, because the relative standard deviation (RSD) was between 2.560% and 4.290% for the EMFP system. In order to highlight the performance of the sensor established in this study, a comparison of IgE detection sensors according to their analytical performances was conducted, as shown in Table 2. The total assay time for the system was 75 min in this study (60 min for immunomagnetic separation, and 15 min for release and measurement), which is superior to most detection times except for at 30 min, whereas the limit of detection of 0.0159 ng mL^{-1} in the present study is the best among the reviewed studies.[23,25,26,28,30,45–47] In particular, one article used a similar

Table 1 sIgE antibody concentrations from nine serum samples as measured by ELISA kits and the EMFP system[a]

Serum number	Commercial ELISA kit value		EMFP system value[b]	
	(ng mL^{-1})	RSD (%)	(ng mL^{-1})	RSD (%)
1	1.997	4.952	2.193	3.466
2	3.228	3.934	4.128	3.506
3	4.034	2.333	5.221	4.290
4	5.723	3.390	6.518	2.946
5	BLOD	—	BLOD	—
6	BLOD	—	0.092	2.348
7	6.613	3.160	7.148	2.560
8	5.113	4.049	5.726	2.655
9	8.476	4.567	9.216	2.717

[a] BLOD means the concentration of sIgE for Meta. E. is below the LOD.
[b] Calculated value using the logistic function above.

Table 2 Comparison of the analytical parameters for IgE detection obtained in this study and reported by previous studies[a]

Detection method	Labels	LOD (ng mL^{-1})	Detection period (min)	Reference
Radioimmunometric	Isotope	0.05		26
ImmunoCAP ISAC	HRP	0.24	150	23
Fluorescent	Photonic crystal	0.048		48
Fluorescent	Gold nanoparticles	0.2	270	28
Chemiluminescent	HRP	300	240	47
Nanoplasmonic	Gold nanodisk	0.6	30	49
Fluorescent	Streptavidin	60	150	47
Electrochemical	Aptamers	>300		50
Fluorescent	FHMNs	0.0159	75	This work

[a] HRP: horse radish peroxidase.

strategy whereby fluorescent microspheres were used as carriers to capture IgE and simultaneously quantify the concentration of IgE.[47] In contrast, in the present study, fluorescent hollow mesoporous nanospheres were utilized to amplify signal from the target IgE in addition to magnetic nanoparticles to rapidly capture and separate the targeted IgE. Moreover, although the previous study applied a fluorescent suspension array to simultaneously detect total IgE and specific IgE, this required substantial time because of the tedious steps. Moreover, the sensitivity was less than that of the EMFP, owing to the high efficiency of EMFP for separation and enrichment of the target sIgE *via* a one-step process, which also markedly simplified the operation and considerably shortened the reaction time. Together, these results indicate that the sensor has high potential for sensitive, reproducible, rapid, and low-cost detection that is simple to process for the determination of sIgE in human sera.

Conclusion

In this study, bio-conjugated FHMNs were developed with the function of signal amplification, and magnetic particles were

synthesized to separate and enrich target sIgE in one step. The sensor composed of these materials was first developed to sensitively test sIgE of Meta. E. from 0.0125 to 9.895 ng mL^{-1} with a LOD of 0.0159 ng mL^{-1}, which is 15-fold more sensitive than that of the FDA-approved ImmunoCAP analyzers. The sensor also exhibits high sensitivity compared with the commercial ELISA; the deviation of sIgE detection levels between these systems might be attributed to the differences in allergen activity after binding, surface chemistry, fluorescence reporter, and detection instrument. In addition, the analytic process of the EMFP system can be completed within 75 min, which is better than the 240 min minimum required for ELISA systems, which might be due to the efficient separation and enrichment of the target sIgE in one step effected by the magnetic nanoparticles, and the simplification of the experimental procedure making it easy to handle. Furthermore, the cheaper materials, reagents, and economical detection equipment renders this system more affordable for developing nations. This methodology could also be readily adapted for detecting other allergies by using different allergen-specific bioelements. The application of nanomaterials to immune detection thus has considerable significance for medical development.

Conflicts of interest

There are no conflicts of interest to declare.

Acknowledgements

References

1 G. du Toit, T. Tsakok, S. Lack and G. Lack, *J. Allergy Clin. Immunol.*, 2016, **137**, 998–1010.

2 K. J. Allen and J. J. Koplin, *Immunol. Allergy Clin. North Am.*, 2012, **32**, 35.

3 A. Muraro, T. Werfel, K. Hoffmann-Sommergruber, G. Roberts, K. Beyer, C. Bindslev-Jensen, V. Cardona, A. Dubois, G. duToit, P. Eigenmann, M. Fernandez Rivas, S. Halken, L. Hickstein, A. Host, E. Knol, G. Lack, M. J. Marchisotto, B. Niggemann, B. I. Nwaru, N. G. Papadopoulos, L. K. Poulsen, A. F. Santos, I. Skypala, A. Schoepfer, R. Van Ree, C. Venter, M. Worm, B. Vlieg-Boerstra, S. Panesar, D. de Silva, K. Soares-Weiser, A. Sheikh, B. K. Ballmer-Weber, C. Nilsson, N. W. de Jong, C. A. Akdis and E. F. A. Anaphylaxis, *Allergy*, 2014, **69**, 1008–1025.

4 S. H. Sicherer and H. A. Sampson, *J. Allergy Clin. Immunol.*, 2014, **133**, 291.

5 B. I. Nwaru, L. Hickstein, S. S. Panesar, A. Muraro, T. Werfel, V. Cardona, A. E. J. Dubois, S. Halken, K. Hoffmann-Sommergruber, L. K. Poulsen, G. Roberts, R. Van Ree, B. J. Vlieg-Boerstra, A. Sheikh and E. F. A. A. Gui, *Allergy*, 2014, **69**, 62–75.

6 R. J. Rona, T. Keil, C. Summers, D. Gislason, L. Zuidmeer, E. Sodergren, S. T. Sigurdardottir, T. Lindner, K. Goldhahn, J. Dahlstrom, D. McBride and C. Madsen, *J. Allergy Clin. Immunol.*, 2007, **120**, 638–646.

7 C. L. Gray, *Curr. Allergy Asthma Rep.*, 2017, **17**, 35.

8 L. Polloni, A. DunnGalvin, E. Ferruzza, R. Bonaguro, F. Lazzarotto, A. Toniolo, N. Celegato and A. Muraro, *Allergy*, 2017, **72**, 1054–1060.

9 J. A. Lieberman and S. H. Sicherer, *Curr. Allergy Asthma Rep.*, 2011, **11**, 58–64.

10 I. Randhawa, C. P. Parrish and T. Morphew, *J. Allergy Clin. Immunol.*, 2016, **137**, AB399.

11 S. H. Sicherer, R. A. Wood and I. Section Allergy, *Pediatrics*, 2012, **129**, 193–197.

12 S. Wahyuni, R. Van Ree, A. Mangali, T. Supali, M. Yazdanbakhsh and E. Sartono, *Parasite Immunol.*, 2003, **25**, 609–614.

13 D. Ferastraoaru, M. Shtessel, E. Lobell, G. Hudes, D. Rosenstreich and G. de Vos, *Am. J. Rhinol. Allergy*, 2017, **8**, 53–62.

14 S. J. Galli and M. Tsai, *Nat. Med.*, 2012, **18**, 693–704.

15 E. S. Unal, U. Gul, A. B. Dursun and F. Oner Erkekol, *Turk. J. Med. Sci.*, 2017, **47**, 577–582.

16 P. J. Howanitz, *Arch. Pathol. Lab. Med.*, 2005, **129**, 1252–1261.

17 P. C. Turkeltaub and P. J. Gergen, *J. Allergy Clin. Immunol.*, 1989, **84**, 886–890.

18 M. L. Kowalski, I. Ansotegui, W. Aberer, M. Al-Ahmad, M. Akdis, B. K. Ballmer-Weber, K. Beyer, M. Blanca, S. Brown, C. Bunnag, A. C. Hulett, M. Castells, H. H. Chng, F. De Blay, M. Ebisawa, S. Fineman, D. B. K. Golden, T. Haahtela, M. Kaliner, C. Katelaris, B. W. Lee, J. Makowska, U. Muller, J. Mullol, J. Oppenheimer, H.-S. Park, J. Parkerson, G. Passalacqua, R. Pawankar, H. Renz, F. Rueff, M. Sanchez-Borges, J. Sastre, G. Scadding, S. Sicherer, P. Tantilipikorn, J. Tracy, V. van Kempen, B. Bohle, G. W. Canonica, L. Caraballo, M. Gomez, K. Ito, E. Jensen-Jarolim, M. Larche, G. Melioli, L. K. Poulsen, R. Valenta and T. Zuberbier, *World Allergy Organ. J.*, 2016, **9**, 33.

19 U. Pipkorn, A. Hammarlund and L. Enerback, *Clin. Exp. Allergy*, 1989, **19**, 19–25.

20 H. A. Sampson and D. G. Ho, *J. Allergy Clin. Immunol.*, 1997, **100**, 444–451.

21 M. Yazdanbakhsh, P. G. Kremsner and R. van Ree, *Science*, 2002, **296**, 490–494.

22 I. J. Wang, W. J. J. Karmaus and C.-C. Yang, *J. Exposure Sci. Environ. Epidemiol.*, 2017, **27**, 478–483.

23 R. G. Hamilton and P. B. Williams, E. T. T. F. Specific Ig and A. Amer Coll, *J. Allergy Clin. Immunol.*, 2010, **126**, 33–38.

24 K. W. Lee, K. Blankenship, B. McKinney, G. Kern, J. Buch, J. Greenwood, P. Brazis, L. Drouet, C. Tambone, R. Faas and G. Weaver, *J. Vet. Diagn. Invest.*, 2015, **27**, 461–469.

25 E. E. Morgan, W. H. Miller Jr and B. Wagner, *Vet. Immunol. Immunopathol.*, 2007, **120**, 160–167.

26 L. K. Poulsen, H. J. Malling, I. Sondergaard and B. Weeke, *J. Immunol. Methods*, 1986, **92**, 131–136.

27 D. Jiang, P. Zhu, H. Jiang, J. Ji, X. Sun, W. Gu and G. Zhang, *Biosens. Bioelectron.*, 2015, **70**, 482–490.

28 M. Cruz Alonso, L. Trapiella-Alfonso, J. M. Costa Fernandez, R. Pereiro and A. Sanz-Medel, *Biosens. Bioelectron.*, 2016, **77**, 1055–1061.

29 E. Ng, K. C. Nadeau and S. X. Wang, *Biosens. Bioelectron.*, 2016, **80**, 359–365.

30 Y. Tan, J. F. Halsey, T. Tang, S. Vande Weteringc, E. Taine, M. Van Cleve and B. T. Cunningham, *Biosens. Bioelectron.*, 2016, **77**, 194–201.

31 I. Moneo, N. Carballeda-Sangiao and M. Gonzalez-Munoz, *Curr. Allergy Asthma Rep.*, 2017, **17**, 27.

32 M. Ben-Shoshan, D. W. Harrington, L. Soller, J. Fragapane, L. Joseph, Y. St Pierre, S. B. Godefroy, S. J. Elliot and A. E. Clarke, *J. Allergy Clin. Immunol.*, 2010, **125**, 1327–1335.

33 S. Tsabouri, M. Triga, M. Makris, D. Kalogeromitros, M. K. Church and K. N. Priftis, *Pediatr. Allergy Immunol.*, 2012, **23**, 608–615.

34 G. Qi, Y. Wang, L. Estevez, A. K. Switzer, X. Duan, X. Yang and E. P. Giannelis, *Chem. Mater.*, 2010, **22**, 2693–2695.

35 R. Cui, C. Liu, J. Shen, D. Gao, J.-J. Zhu and H.-Y. Chen, *Adv. Funct. Mater.*, 2008, **18**, 2197–2204.

36 M. L. Kang, J.-Y. Ko, J. E. Kim and G.-I. Im, *Biomaterials*, 2014, **35**, 9984–9994.

37 R.-R. Hu, Z.-Z. Yin, Y.-B. Zeng, J. Zhang, H.-Q. Liu, Y. Shao, S.-B. Ren and L. Li, *Biosens. Bioelectron.*, 2016, **78**, 31–36.

38 Q. Dang Viet, J. E. Lee, J.-K. Kim, Y. N. Kim, G. N. Shao and H. T. Kim, *Powder Technol.*, 2013, **235**, 221–227.

39 J.-L. Gong, X.-Y. Wang, G.-M. Zeng, L. Chen, J.-H. Deng, X.-R. Zhang and Q.-Y. Niu, *Chem. Eng. J.*, 2012, **185**, 100–107.

40 J. Li, Q. Li, Y. Zeng, T. Tang, Y. Pan and L. Li, *RSC Adv.*, 2015, **5**, 717–725.

41 B. Fotoohi and L. Mercier, *Hydrometallurgy*, 2015, **156**, 28–39.

42 R. El-kharrag, A. M. R. Amin and Y. E. Greish, *Ceram. Int.*, 2012, **38**, 627–634.

43 G. Qi, Y. Wang, L. Estevez, A. K. Switzer, X. Duan, X. Yang and E. P. Giannelis, *Chem. Mater.*, 2010, **22**, 2693–2695.

44 H. J. Chen, Y. L. Wang, Y. Z. Wang, S. J. Dong and E. K. Wang, *Polymer*, 2006, **47**, 763–766.

45 G. Wang, X. Su, S. Yang, Y. Jia and D. Li, *J. Lumin.*, 2012, **132**, 2505–2511.

46 X. Wang, P. Wang, R. Fan, M. Xu, L. Qiang, L. Wei, Y. Yang and Y. Wang, *Dalton Trans.*, 2015, **44**, 5179–5190.

47 E. M. King, L. D. Vailes, A. Tsay, S. M. Satinover and M. D. Chapman, *J. Allergy Clin. Immunol.*, 2007, **120**, 1126–1131.

48 Y. F. Tan, J. F. Halsey, T. T. Tang, S. Vande Weteringc, E. Taine, M. Van Cleve and B. T. Cunningham, *Biosens. Bioelectron.*, 2016, **77**, 194–201.

49 M. Soler, P. Mesa-Antunez, M. Estevez, A. Ruiz-Sanchez, M. Otte, B. Sepulveda, D. Collado, C. Mayorga, M. Torres, E. Perez-Inestrosa and L. Lechuga, *Biosens. Bioelectron.*, 2015, **66**, 115–123.

50 K. Papamichael, M. Kreuzer and G. Guilbault, *Sens. Actuators, B*, 2007, **121**, 178–186.